

Transport properties of β -Ga₂O₃ Nanoparticles embedded in Nb thin films

L.S.Vaidhyanathan^{a*}, M.P. Srinivasan^b, P. Chandra Mohan^b, D.K. Baisnab^a R. Mythili^c
and M.P. Janawadkar^a

^aCondensed Matter Physics Division, Indira Gandhi Centre for Atomic Research,
Kalpakkam, India.

^b Water and Steam Chemistry Division, Bhabha Atomic Research Centre Facilities,
Kalpakkam, India

^c Microscopy & Thermo-Physical Property Division,, Indira Gandhi Centre for Atomic
Research, Kalpakkam, India.

Abstract

The origin of ferromagnetism in nanoparticles of nonmagnetic oxides is an interesting area of research. In the present work, transport properties of niobium thin films, with β -Ga₂O₃ nanoparticles embedded within them, are presented. Nanoparticles of β -Ga₂O₃ embedded in a Nb matrix were prepared at room temperature by radio frequency co-sputtering technique on Si (100) and glass substrates held at room temperature. The thin films deposited on Si substrates were subjected to Ar annealing at a temperature range of 600-650 C for 1 hour. Films were characterized by X-ray diffraction (XRD), Micro-Raman and elemental identification was performed with an Energy Dispersive X-ray Spectroscopy (EDS). Transport measurements were performed down to liquid helium temperatures by four-probe contact technique, showed characteristics analogous to those observed in the context of a Kondo system. A comparison of the experimental data with the theoretical formalism of Kondo and Hamann is presented. It is suggested that this behavior arises from the existence of magnetic moments associated with the oxygen vacancy defects in the nanoparticles of the nonmagnetic oxide Ga₂O₃.

* Corresponding author: Telefax: 0091-44-27480081;

Email address: lsv@igcar.gov.in (L.S. Vaidhyanathan)

Key words: A. Thin films; B. Sputtering; C. SEM with EDS; D. Kondo effect.

1. Introduction

The Kondo effect which is characterized by $\log T$ behaviour in the temperature dependence of electrical resistivity at low temperatures, has been the subject of extensive theoretical and experimental research. It has been studied in both crystalline [1] and amorphous [2] systems with the introduction of magnetic impurities carrying a magnetic moment. Recent experiments have lent credence to the existence of a new fundamental state of magnetism, viz “Quantum Spin Liquid” [3] and Anderson, who first proposed this concept, has explored its relevance in the context of High temperature Superconductivity [4]. The topic related to the interaction of superconductivity with magnetism is of great theoretical and experimental interest and there are many interesting problems which are at the frontiers of current research. The experimental investigations range from studies on proximity effect in superconductor (S)-ferromagnet (F) bilayers, SFS trilayers, spin injection into the superconductors, π type superconductivity etc. On the theoretical side, in SF structures existence of spatial modulation of the superconducting pair potential is envisaged and exotic phenomenon of spin triplet superconductivity in SFS system is anticipated. Room temperature ferromagnetism has been recently observed in nanoparticles of several nonmagnetic oxides [5] and the origin of ferromagnetism is still a matter of debate. Ga_2O_3 is an exclusive deep ultraviolet transparent conducting oxide and it has interesting electrical conductivity characteristics, such as the high electrical conductivity of $\sim 40 \text{ S cm}^{-1}$ induced by tin doping [6]. An insulator to metal transition with a conductivity enhancement of seven orders of magnitude [7] has been observed in amorphous non-stoichiometric Gallium oxide thin films and has been explained as arising due to heterogeneous solid state reaction.

In view of this, it would be interesting to investigate the effect of Ga_2O_3 on the superconducting properties of materials such as Nb. This paper reports the investigations on the electrical transport properties of $\text{Ga}_2\text{O}_3/\text{Nb}$ thin films, especially after post annealing the film under reducing conditions at elevated temperatures, and the experimental data has been analyzed using the theoretical formalism proposed by Kondo and Hamann [8].

2. Experiments

Nanoparticles of β -Ga₂O₃ embedded in a Nb matrix were prepared at room temperature by radio frequency co-sputtering technique after establishing a base pressure of 1.3×10^{-7} mbar. Nb target of 99.99% purity and ultra high pure Ar gas (99.9995%) were used to deposit the thin films. Ga₂O₃ nanoparticles were formed in a Nb matrix by co-sputtering a Nb target (10 cm diameter) along with 2 cm diameter target of Ga₂O₃ to deposit the thin film on Si (100) and glass substrates held at room temperature. The composite films of thickness of 200 nm were deposited in the presence of ultra high pure Ar gas at a pressure of 8 mTorr with incident RF power of 90 W. Electrical contacts to the thin films were provided in the standard four probe contact geometry using UV photolithography. The thin films deposited on Si substrates were subjected to annealing in argon atmosphere by keeping the films in ultra high pure Argon gas at a pressure of 15 mbar at two different temperatures (a) T = 600 C for 30 minutes (batch – I) and (b) T = 650 C for 60 minutes (batch – II). The crystal structure and orientation of the thin films were characterized by X-ray diffraction (XRD) measurements in a STOE diffractometer using CuK_α radiation. Micro-Raman study is a sensitive technique to probe the local atomic environments and here Confocal Dispersive Raman microscopy with Argon ion laser (514.5nm) was used for acquiring the spectra from the sample surface in the back scattering mode. The elemental identification of Nb-Ga₂O₃ thin films on glass substrates was carried out using Philips XL- 30 SEM fitted with an Energy Dispersive X-ray Spectroscopy (EDS). Transport measurements were performed down to liquid helium temperatures by four-probe contact technique using indium soldering to establish the contacts.

3. Results and Discussion

Fig. 1a shows the room temperature GIXRD pattern of Nb-Ga₂O₃ film using CuK_α radiation showing (110), (200) and (211) Bragg peaks corresponding to only Nb. No lines corresponding to the Ga₂O₃ phase could be detected since the volume fraction of Ga₂O₃ in the film estimated from the deposition rates is less than the detection limit for

XRD of 5 % Fig. 1b shows the room temperature Raman spectra recorded from Nb-Ga₂O₃ thin film prepared on borosilicate glass substrate. The peak at 200 cm⁻¹ arises from the different vibrational modes of β- Ga₂O₃ and the peak at 806 cm⁻¹ is ascribed to symmetric stretching motions of silica tetrahedra with oxygen in the borosilicate glass [9]. It is generally seen in literature that the detection of Raman spectrum from a metal (like Nb) is beset with lot of difficulties. Fig. 1c shows the EDS spectra showing the elemental identity of Nb and Ga through their characteristic X-ray energies. The other element such as Ca is also observed due to glass substrate.

The temperature variation of electrical resistivity $\rho(T)$ of Ar annealed Nb-Ga₂O₃ thin film (batch -I) is shown in Fig. 2 for the temperature range between 5 K to 210 K. The electrical resistivity has a value of $\sim 80 \mu\Omega \text{ cm}$ at 210 K, increases with decrease in temperature, exhibits a broad maximum around 50 K and then decreases with further decrease in temperature. The top inset shows the schematics of film deposition and measurement performed. The inset at the bottom shows the variation of $\rho(T)$ of the as deposited Nb-Ga₂O₃ thin film which exhibits a normal metallic behaviour with decrease in temperature but is not superconducting down to 4.2 K. An rough estimate of the particle size of Nb using Scherrer formula turns out to be 10 nm. The nanostructured Nb thin films of size of $\sim 10 \text{ nm}$ does not show superconducting behaviour. Added to it, the Presence of Ga₂O₃ nanoparticles dispersed in niobium may have the potential to radically alter the conduction behaviour as well as superconductivity.

Similarly, the temperature dependence of the electrical resistivity $\rho(T)$ of batch - II sample of Ar annealed Nb-Ga₂O₃ thin film is shown in Fig. 3. It may be noted that $\rho(T)$ for this specimen also increases with decrease in temperature with an eventual saturation of $\rho(T)$ at temperatures between 35K and 4.2K. Our analysis of the experimental data is based on the observation of magnetism in nanoparticles of several non-magnetic oxides such as Al₂O₃, SnO₂, In₂O₃ etc [5]

A characteristic feature of Kondo system is the observation of a resistance minimum with a logarithmic divergence of resistivity at lower temperatures. It is well known that when

the exchange interaction between the magnetic moment of the impurity and the conduction electron spins is antiferromagnetic, the contribution to the electrical resistivity arising from spin flip scattering varies as $\ln T$.

$$\rho(T) = (\rho_o + \rho_o^\infty) - a_K \ln T \quad (1)$$

here, ρ_o is the contribution from the scattering of the conduction electrons with lattice defects, while ρ_o^∞ is that due to non spin flip scattering. The second term accounts for Kondo effect viz., spin flip scattering of the conduction electrons by the magnetic moments

The temperature variation of electrical resistivity $\rho(T)$ of Ar annealed Nb-Ga₂O₃ thin film (batch –I) is fitted with eqn.1. A good fit to the data (Fig. 2) is obtained for temperatures above 75 K and is shown as a solid line in Fig. 2 with the fitting parameters $(\rho_o + \rho_o^\infty) = 90 \mu\Omega \text{ cm}$ and $a_K = 2.2 \mu\Omega \text{ cm}$. (Table I)

The temperature variation of electrical resistivity $\rho(T)$ for Nb-Ga₂O₃ thin film (batch –II), which was subjected to Argon annealing for a longer duration of time, was also fitted to eqn.1 and the results are shown in Fig. 3 (inset). A good fit to the data could, however, be obtained only in the temperature range above 235 K to room temperature and is shown as a solid line with the fitting parameters $(\rho_o + \rho_o^\infty) = 880 \mu\Omega \text{ cm}$ and $a_K = 130 \mu\Omega \text{ cm}$ (Table I).

It may be noted that at low temperatures, the electrical resistivity ρ deviates from the expected $\ln T$ behaviour and begins to saturate at lower temperatures. To further analyze the resistivity, the experimental data of the thin films of batch –II is fitted to the expression given by Hamann [8]

$$\rho_{sd} = \frac{\rho_o}{2} \left(1 - \frac{\ln(T/T_{KO})}{\left(\ln^2(T/T_{KO}) + S(S+1)\pi^2 \right)^{1/2}} \right) \quad (2)$$

Hamann has shown that, similar to the anomalous conduction electron scattering enunciated by Kondo from the s-d exchange model, the Anderson extra orbital dilute alloy model is also of value in accounting for the experimentally observed resistivity behaviour. In eq.2. T_{K_0} is the Kondo temperature and S is the impurity spin value and ρ_0 is the unitarity limit. Resistivity ρ of the sample is represented by $\rho = \rho_{sd} + \langle B \rangle$, where $\langle B \rangle$ is the temperature independent contribution to the resistivity to account for the potential scattering background. The parameters T_{K_0} , ρ_0 and $\langle B \rangle$ are varied to fit the experimental values for ρ as per eqn.2 are shown in Fig. 3 and the values of the fitting parameters have been tabulated in Table I .

One of the characteristic features of Kondo system is the occurrence of plateau of resistivity at low temperatures. Typically saturation starts at $\sim 0.1 T_{K_0}$. If $T_{K_0} \sim 300$ K, saturation will roughly set in at $T \sim 30$ K. One can see from Fig. 3 that such a plateau of resistivity is seen at $T \leq 30$ K. In order to understand the low temperature saturation of resistivity as seen in Fig. 3 for the Ar annealed Nb-Ga₂O₃ thin film sample of batch-II, the resistivity measured for the as deposited Nb-Ga₂O₃ (without any annealing) was subtracted and plotted in Fig. 4. A very good fit for the entire temperature range to the experimental data was obtained and the fitting parameters are shown in Table I.

Both Kondo and Hamann theories make definite predictions for the temperature dependence of electrical resistivity at low temperatures. The Kondo effect has been experimentally observed in several systems which also include amorphous alloys. For example, the introduction of the magnetic impurities such as Cr into an amorphous alloy of Ni₄₁Pd₄₁B₁₈ was seen to affect the transport properties and revealed a characteristic logarithmic temperature dependence of resistivity [10]. It is also customary in these studies to separate out the magnetic contribution from the parent compound to study the temperature dependence of resistivity [11]. However, the system Nb-Ga₂O₃ is interesting because both Nb and Ga₂O₃ are known to be nonmagnetic in bulk. However, the possibility of magnetism in several nonmagnetic oxides is being actively investigated in the current literature [12-13] with a view to understand the origin of magnetism in such oxides and its influence on the physical properties. It is speculated that the origin of

magnetism in such nonmagnetic oxides may arise from the localized electron spin moments ensuing from the oxygen vacancies at the surfaces of nanoparticles of these materials. In the present work, transport properties of as deposited Nb-Ga₂O₃ thin films exhibited the normal metallic behaviour from room temperature down to ~ 30 K while Ar annealed thin films of Nb-Ga₂O₃ exhibited a non-metallic behaviour and revealed a characteristic $\ln T$ temperature dependence at low temperatures probably due to the existence of localized magnetic moments associated with the oxygen vacancy defects. Indeed, the experimentally observed behaviour of the temperature dependence of electrical resistivity showing Kondo-like anomaly lends credence to the existence of magnetic moments in this system. Although challenging, it would be of interest to study the temperature dependence of magnetic susceptibility to throw light on presence of magnetic moments in this system.

4. Conclusion

In summary, β -Ga₂O₃ nanoparticles embedded in Nb thin films were deposited by RF magnetron sputtering. For Nb/Ga₂O₃ thin films annealed in Argon atmosphere, the temperature dependence of electrical resistivity at low temperatures showed characteristics analogous to those observed in a Kondo system. The experimental data have been analyzed using the theoretical formalism proposed by Kondo and Hamann, which predict a characteristic logarithmic temperature dependence of resistivity at low temperatures. The experimentally observed behavior of electrical resistivity is in broad agreement with these predictions, pointing to the existence of magnetic moments at oxygen vacancy defects in the nanoparticles of these nonmagnetic oxides.

Acknowledgements

The authors would like to thank Dr V. Sridharan for the help in providing the Ga₂O₃ sample. Thanks are due to Ms Kalavathi for help in X-ray measurements. We thank

Dr C.S. Sundar, Director MSG, for his interest in our work. We acknowledge the support received from IGCAR during the execution of this work.

References

- [1] J. Kondo, Solid State Physics (F.Seitz and D.Turnbull, Eds., Academic Press), **23** (1969) 183
- [2] R. Hasegawa and C.C. Tsuei Phys Rev **B 2** (1970) 1631
- [3] Tian-Heng Han, Joel S. Helton, Shaoyan Chu, Daniel G. Nocera; Jose A. Rodriguez-Rivera, Collin Broholm & Young S.Lee Nature **492** (2012) 406
- [4] P.W. Anderson, Science **235** (1987) 1196
- [5] A. Sundaresan, R. Bhargavi, N. Rangarajan, U. Siddesh & C.N.R. Rao Phys Rev **B 74** (2006) 161306 (R)
- [6] N.Ueda, H. Hosono, R.Waseda and H. Kawazoe Appl.Phys.Lett. **70** (1997) 3561
- [7] Lakshmi.Nagarajan, Roger A. De Souza, Dominik Samuelis, Ilia Valov, Alexander Boerger, Juergen Janek, Klaus-Dieter Becker, Peter C. Schmidt & Manfred Martin Nature Materials **7** (2008) 391
- [8] D.R. Hamann Phys Rev **158** (1967) 570
- [9] William B. White and David G. Minser J.Non Crystalline Solids **67** (1984) 45
- [10] V.K.C. Liang and C.C. Tsuei Phys Rev **B 7** (1973) 3215
- [11] A. Kowalczyk, V.H.Tran, T.Tolinski & W.Miiller Solid.Stat.Comm. **144** (2007) 185
- [12] J.Osorio-Guillen, S. Lany, S.V.Barabash and A. Zunger Phys. Rev. **B 75** (2007) 184421
- [13] M. Carmen Munoz, S. Gallego and N. Sanchez J. Physics (*Conference Series*) **303** (2011) 012001

Table 1: Fit parameters of temperature variation of electrical resistivity $\rho(T)$ of Ar annealed Nb- Ga₂O₃ thin films

Ar annealed Nb-Ga ₂ O ₃ thin film	Kondo theory	Hamann theory
Bartch-I	$(\rho_0 + \rho_0^\infty) = 90 \mu\Omega \text{ cm}$ $a_K = 2.2 \mu\Omega \text{ cm}$	
Batch-II	$(\rho_0 + \rho_0^\infty) = 880 \mu\Omega \text{ cm}$ $a_K = 130 \mu\Omega \text{ cm}$	$\rho_0 = 90 \mu\Omega \text{ cm}$ $T_{K0} = 299 \text{ K}$ $\langle B \rangle = 70 \mu\Omega \text{ cm}$
$\Delta\rho$ (ρ [Ar annealed Nb-Ga ₂ O ₃ : batch II] – ρ [Nb-Ga ₂ O ₃ as deposited])		$\rho_0 = 130 \mu\Omega \text{ cm}$ $T_{K0} = 315 \text{ K}$ $\langle B \rangle = 9.7 \mu\Omega \text{ cm}$

Figure Captions

Fig. 1. (a) Room temperature GIXRD pattern of Nb-Ga₂O₃ film; (b) Room temperature Raman spectra recorded from Nb-Ga₂O₃ thin film prepared on borosilicate glass substrate; (c) EDS spectra of Nb-Ga₂O₃ thin film prepared on borosilicate glass substrate.

Fig. 2. The temperature variation of electrical resistivity $\rho(T)$ of Ar annealed Nb-Ga₂O₃ thin film (batch –I). The linear variation with $\ln(T)$ at temperatures above 75K (shown by the solid line) indicates Kondo –like behaviour. Inset shows the variation of $\rho(T)$ of the as deposited Nb-Ga₂O₃ thin film (without any annealing); top inset shows the schematics of film deposition and measurement performed.

Fig. 3. Temperature variation of electrical resistivity $\rho(T)$ of Ar annealed Nb-Ga₂O₃ thin film (batch –II). Line denotes a fit due to Hamann’s theory. Inset shows a fit (solid line) to a logarithmic temperature dependence.

Fig. 4. Comparison of Hamann’s theory (solid line) with the $\rho(T)$ data of Ar annealed Nb-Ga₂O₃ thin film (batch – II), after subtracting the electrical resistivity of the as deposited Nb-Ga₂O₃ thin film.

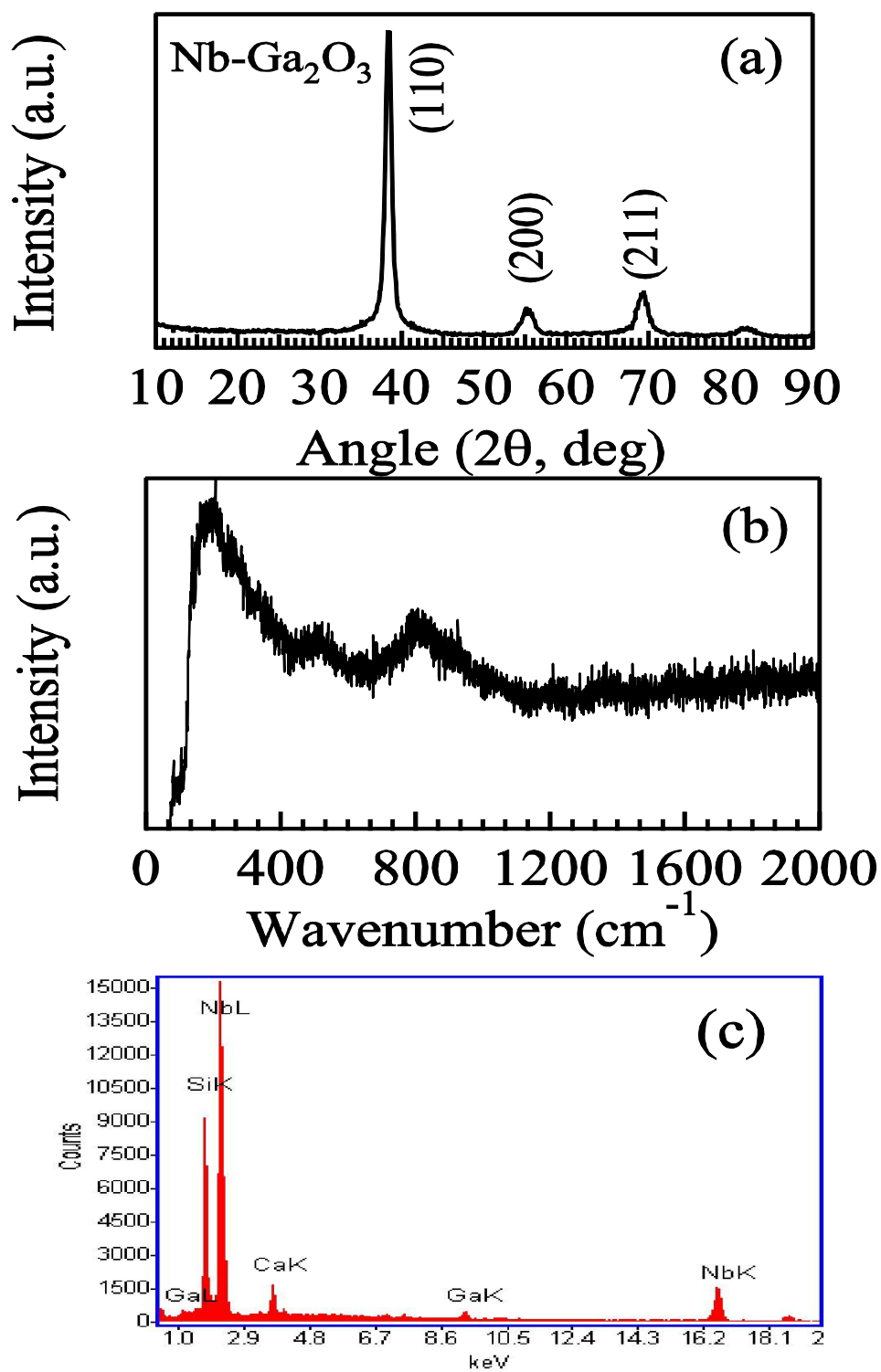


Fig.1.

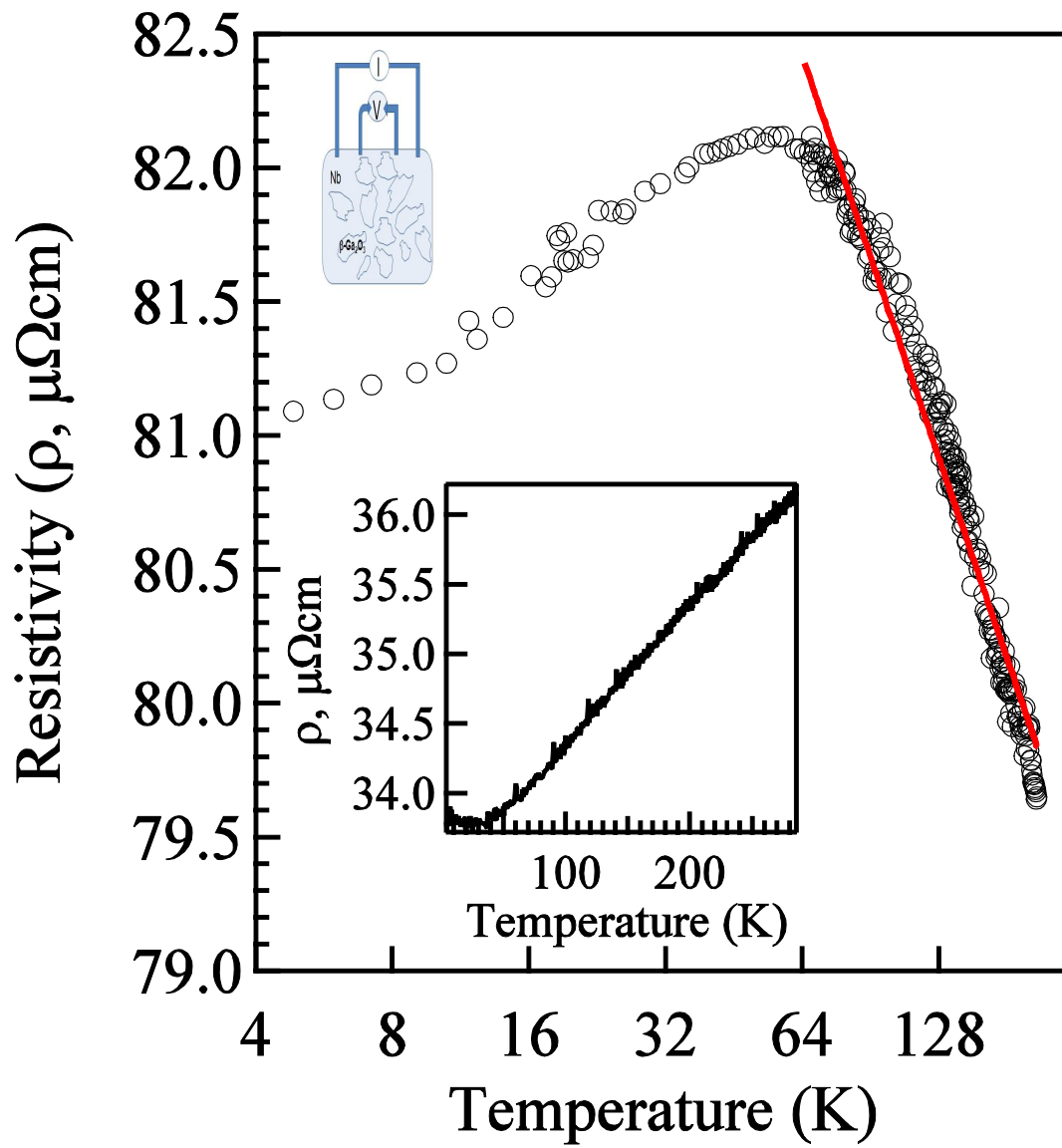


Fig.2.

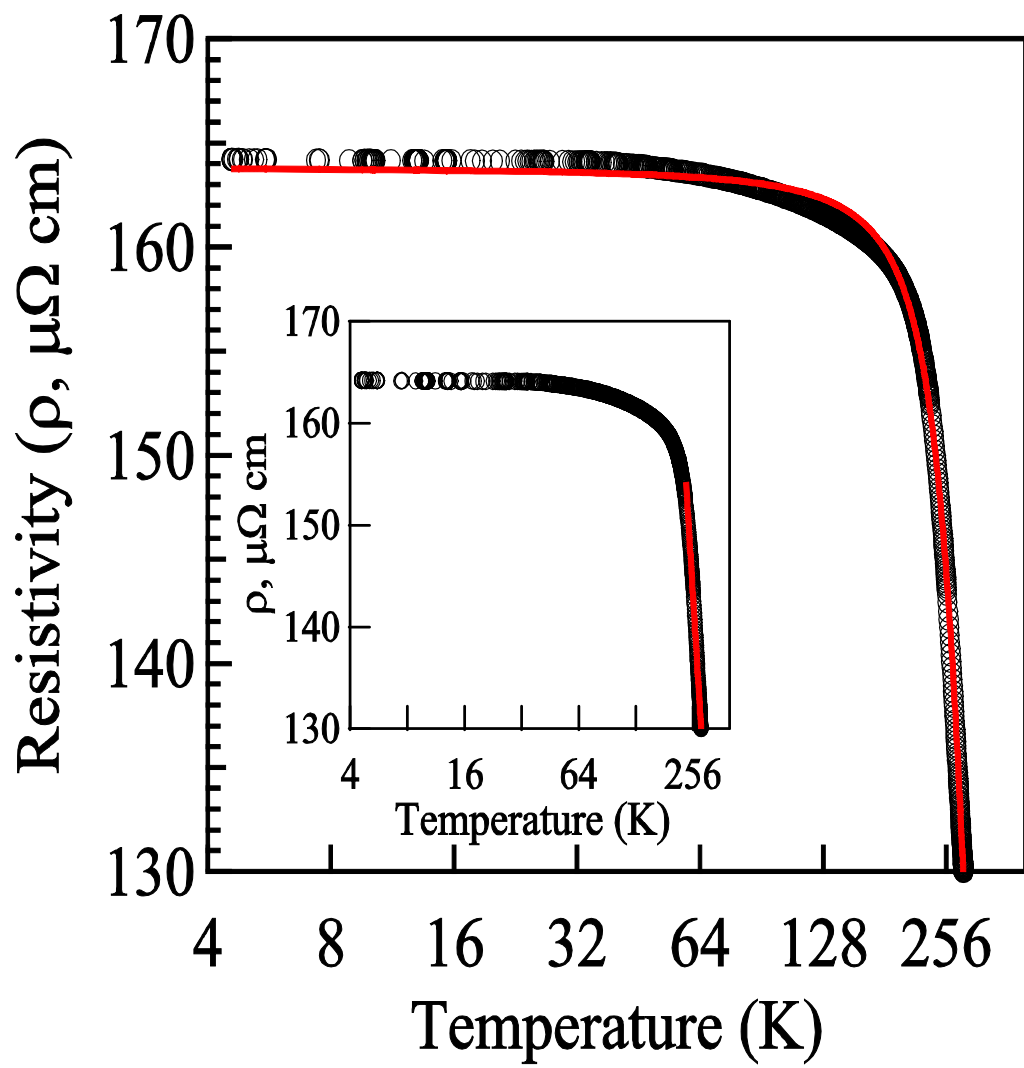


Fig.3.

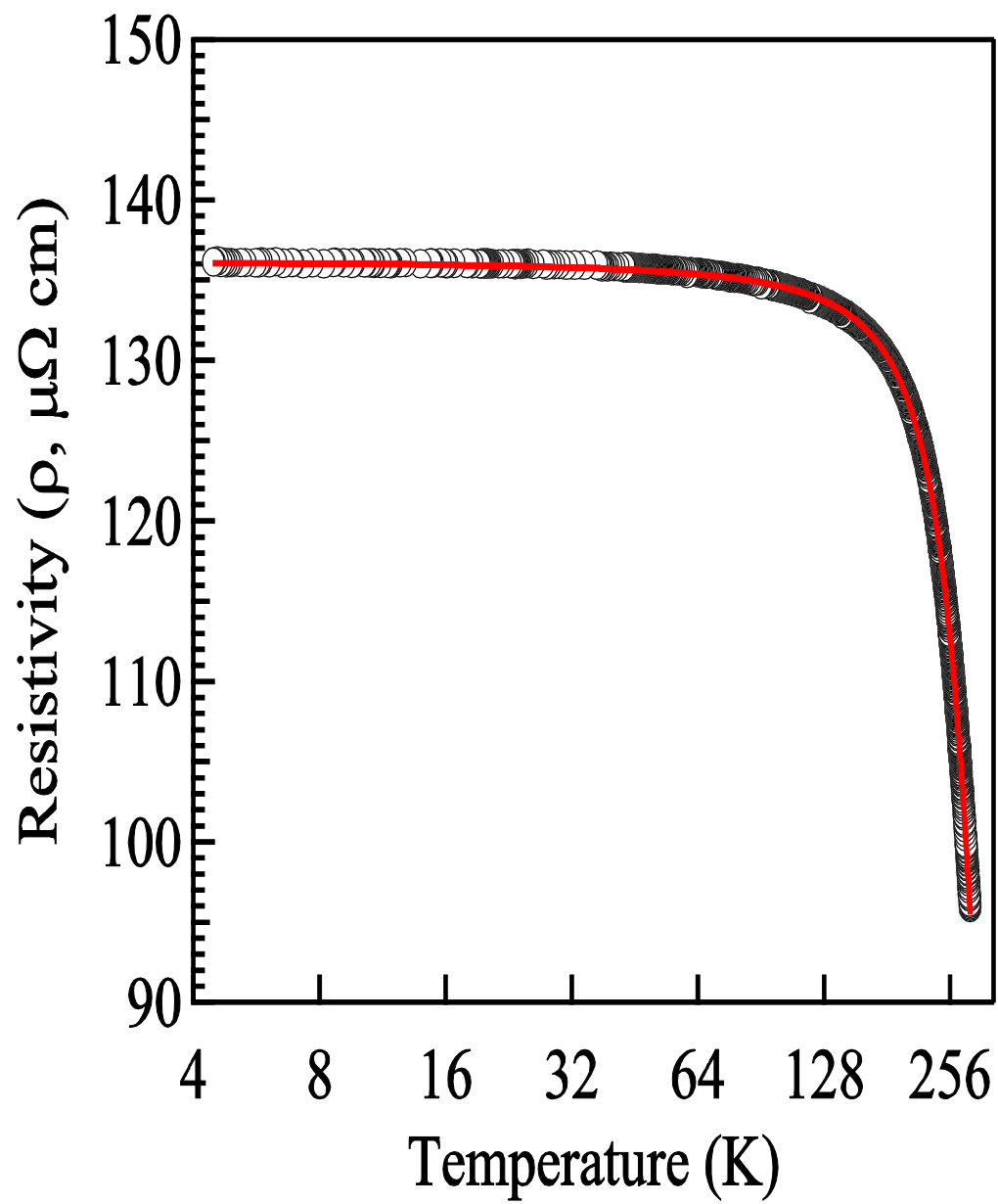


Fig.4.